ISSN 1063-4576, Journal of Superhard Materials, 2014, Vol. 36, No. 4, pp. 246–256. © Allerton Press, Inc., 2014.

PRODUCTION, STRUCTURE, PROPERTIES

Metastable Host–Guest Structure of Carbon[1]

Q. Zhu[a, b, *], O. D. Feya[c], S. E. Boulfelfel[a], and A. R. Oganov[a–d, **]

[a] *Department of Geosciences, State University of New York, Stony Brook, NY 11794-2100*

[b] *Center for Materials by Design, Institute for Advanced Computational Science, State University of New York, Stony Brook, NY 11794-2100*

[c] *Moscow Institute of Physics and Technology, 9 Institutskiy lane, Dolgoprudny city, Moscow Region, 141700, Russian Federation*

[d] *Northwestern Polytechnical University, Xi'an, 710072, P. R. China*

**e-mail: alecfans@gmail.com*
***e-mail: artem.oganov@sunysb.edu*

Received March 15, 2014

Abstract—A family of metastable host–guest structures, the prototype of which is a tetragonal *tP*9 structure with 9 atoms per cell has been found. It is composed of an 8-atoms tetragonal host, with atoms filling channels oriented along the c-axis. The *tP*9 structure has a strong analogy with the recently discovered Ba-IV- and Rb-IV-type incommensurate structures. By considering modulations of the structure due to the variations of the host/guest ratio, it has been concluded that the most stable representative of this family of structures has a guest/host ratio of 2/3 and 26 atoms in the unit cell (space group $P4_2/m$). This structure is 0.39 eV/atom higher in energy than diamond. We predict it to have band gap 4.1 eV, bulk modulus 384 GPa, and hardness 61–71 GPa. Due to the different local environments of the host and guest atoms, we considered the possibility of replacing carbon atoms in the guest sublattice by Si atoms in the *tP*9 prototype and study the properties of the resulting compound SiC_8, which was found to have remarkably high bulk modulus 361.2 GPa and hardness 46.2 GPa.

DOI: 10.3103/S1063457614040030

Keywords: density functional theory, evolutionary algorithm, incommensurate crystal, silicon carbide.

1. INTRODUCTION

Carbon is a unique element in the sense that it adopts a wide range of structures, from superhard insulators (diamond and lonsdaleite) to ultrasoft semimetals (graphite, an excellent lubricant) and even superconductors (intercalated graphite and fullerenes, doped diamond) [1–5]. Among the solid phases, only graphite, diamond and the bC8 phase (predicted to be stable at pressures above 1 TPa) have stability fields on the phase diagram. However, the number of all possible metastable phases is in principle infinite, and due to directional covalent bonding, many metastable carbon phases are known, and have extremely long (technically indefinite) lifetimes. Much work both in experiment and theory has been done to search for novel carbon phases with special properties (such as metallic conductivity, hardness, etc.) [6–17]. Until now, it has not been imagined that carbon could also adopt a host–guest structure.

The nature of host–guest structures of compressed metals is still somewhat puzzling, given their ubiquity and complex and relatively open topologies [18]. Since Ba-IV was first solved experimentally [19, 20], a series of complex phases with composite host–guest structures were found for alkali, alkali earth, group 15 and 16 elements (e.g., [21–29]). Recently, aluminum was also predicted to adopt a similar host–guest type structure at extremely high pressure (about 1 TPa) [30]. To the best of our knowledge, group 14 elements have not been reported to have host–guest structures. However, our structure searches uncovered such structures as metastable states. Although metastable, rather than thermodynamically stable, these are of great interest for the understanding of carbon polymorphism and of the nature of host–guest structures. The newly found structures provide an interesting way of constructing a host–guest network, suitable for low-coordinate atoms and alternative to the known Ba-IV and Rb-IV host–guest structure types.

[1] The text was submitted by the authors in English.

2. COMPUTATIONAL METHODS

Evolutionary structure searches were performed using the USPEX code [31–33] in conjunction with ab initio structure relaxations using density functional theory (DFT) [34, 35] within the Perdew-Burke-Ernzerhof (PBE) generalized gradient approximation (GGA) [36], and the all-electron projector-augmented wave [37, 38] (PAW) method, as implemented in the VASP code [39]. We used a PAW potential with [$1s^2$] core, plane wave kinetic energy cutoff of 600 eV, and Brillouin zone sample with reciprocal space resolution of $2\pi \times 0.05$ Å^{-1}, which ensured excellent convergence of total energies, stresses, and energy differences. These calculations correctly yielded the ground states—graphite at normal conditions, diamond at high pressures, and bc8 at ultrahigh pressures above 1 TPa [31].

To ensure that the obtained structures are dynamically stable, we calculated phonon frequencies across the Brillouin zone using the frozen-phonon method as implemented in the PHONOPY code [40]. For obtaining the electronic density of states (DOS) of the 9-atom *tP*9 and SiC_8 structures we used $5 \times 5 \times 8$ k-points grid for self-consistent calculations, followed by a non-self-consistent calculation with a $10 \times 10 \times 16$ grid, and same-resolution grids for the 26-atom modulated structure. Band structures were calculated using the hybrid functional HSE06 [41]. Bader analysis [42] was performed using the code [43]. We estimated hardnesses using the Lyakhov-Oganov approach [16] and the Chen-Niu model [44]; for the latter, bulk and shear moduli are required—these were computed within the Voigt-Reuss-Hill averaging scheme [45–47] of the elastic constants computed by finite strain method.

3. RESULTS

3.1. Host–Guest Structure of Pure Carbon

We have performed structure searches at 0, 5, 10 GPa with 3, 4, 6, 9, 12 atoms per unit cell, respectively. Apart from the already known structures (diamond, lonsdaleite, bc8, M-carbon, bct4, etc.), our simulations also found a tetragonal host–guest structure. This composite structure is shown in Fig. 1a, and consists of a host sublattice (8 atoms in the unit cell with lattice parameters $a = b = 4.560$ Å and $c = 2.556$ Å). The symmetry of the host sublattice is $P4_2/m$; there are two 4j Wyckoff sites—C_{h1}(0.288, 0.781, 0.223) and C_{h2}(0.839, 0.531, 0.266). The guest atoms occupy the sites C_g(0, 0, 0) and there is only 1 guest atom in the unit cell. The space group of the whole host–guest structure is lowered to *P*4. This structure has strong analogy with well-known Ba-IV and Rb-IV host–guest structure as shown in Figs. 1c, 1d. The main difference is that carbon prefers low coordination numbers (in this structure, C atoms are in a distorted fourfold coordination), while the average coordination number of host and guest atoms is typically 8–10 in Ba-IV or Rb-IV type structures. *tP*9 is a low-coordinate host–guest structure.

Bond lengths within the host sublattice vary between 1.53–1.57 Å, while the shortest host–guest bond is 1.74 Å. Bond angles within the host sublattice are 107°90′ and 119°01′; guest-host bonds form angles 105°73′ and 124°91′. These values are close to the ideal angles of 109°28′ and 120° for sp^3- and sp^2-hybridizations.

To compute the hardness of *tP*9, we used the Lyakhov-Oganov [16] and Chen-Niu [44] models—the results of these completely independent models being very similar, 70.4 and 72.8 GPa, respectively. The bulk

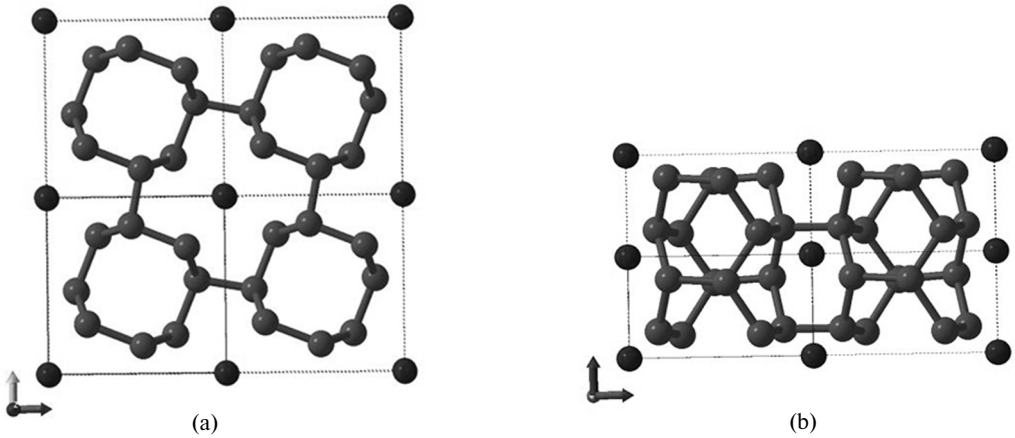

(a) (b)

Fig. 1. Crystal structure of *tP*9-carbon in two projections (a, b); also show are Ba-IV (c) and Rb-IV (d) structure.

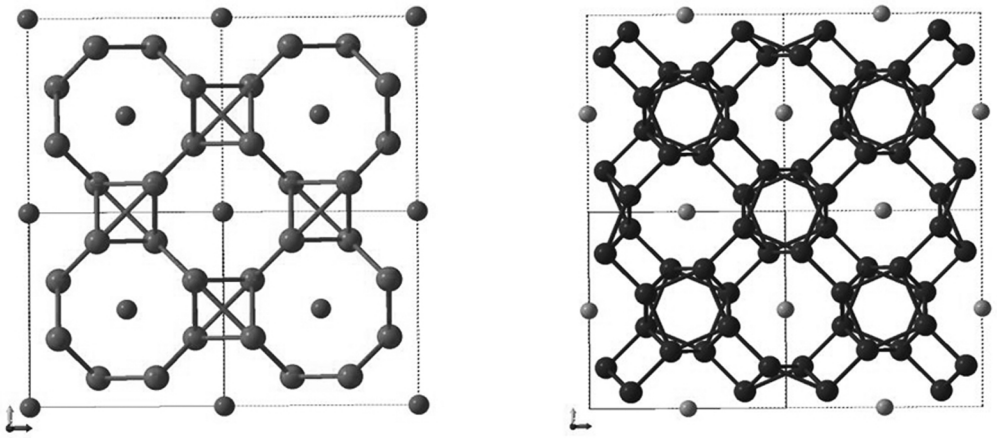

(c) (d)

Fig. 1. (Contd.)

modulus is remarkably high, 388 GPa (for comparison, the bulk modulus of diamond computed at the same level of theory is 431 GPa [15]). Its density is 3.37 g/cm^3.

We have calculated the enthalpies of the host–guest structure and some other well-known and hypothetical structures as a function of pressure (Fig. 2). Our host–guest structure is 0.55 eV/atom higher in energy than diamond at $P = 0$, but more energetically favorable than the predicted superdense allotropes [15]. At the same time, it is dynamically stable (i.e., there are no imaginary phonon frequencies, Fig. 3) and, once synthesized, may exist as a metastable phase. The electronic band structure of *tP*9 is shown in Fig. 4. According to the HSE06 hybrid functional (known to rather accurately estimate the band gaps of carbon allotropes), it is a semiconductor with an indirect band gap of 3 eV at zero pressure.

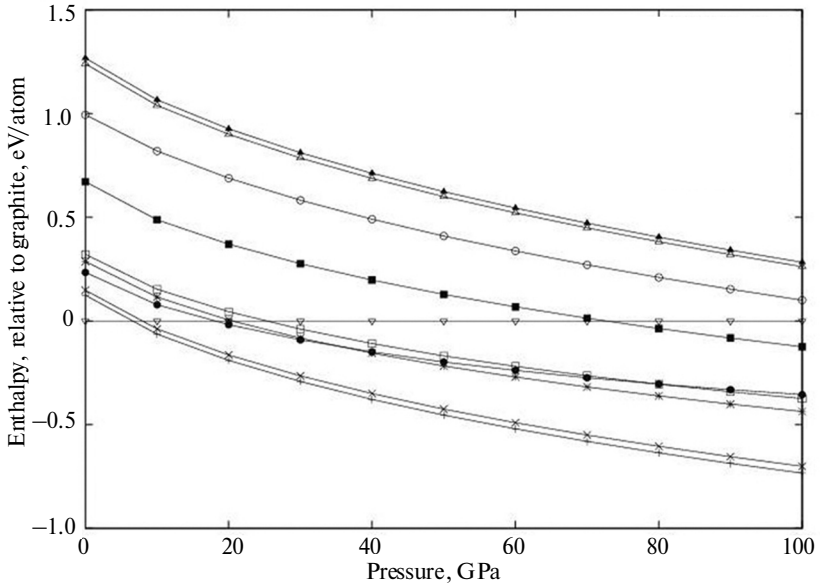

Fig. 2. Enthalpies of various carbon structures, relative to graphite: diamond (+), lonsdaleite (×), M-carbon (∗), bct-4 (□), *tP*9 (■), *tP*12 (○), chiral (●), *hP*3 (△), *tI*12 (▲), graphite (▽).

The geometric difference between host and guest sublattices invites the question of possible charge transfer (as found in γ-boron [48]). We performed Bader analysis of the total charge density of *tP*9-carbon and results are presented in Table 1. As one can see, although different carbon sites have very different local environments and there is a large variation of Bader volumes, charge transfer is quite modest in this structure, and Bader charges are rather small.

In the next section we explore an additional degree of freedom that host–guest structures have, namely the host/guest periodicity ratio. This allows us to obtain a more stable host–guest structure and explore its properties.

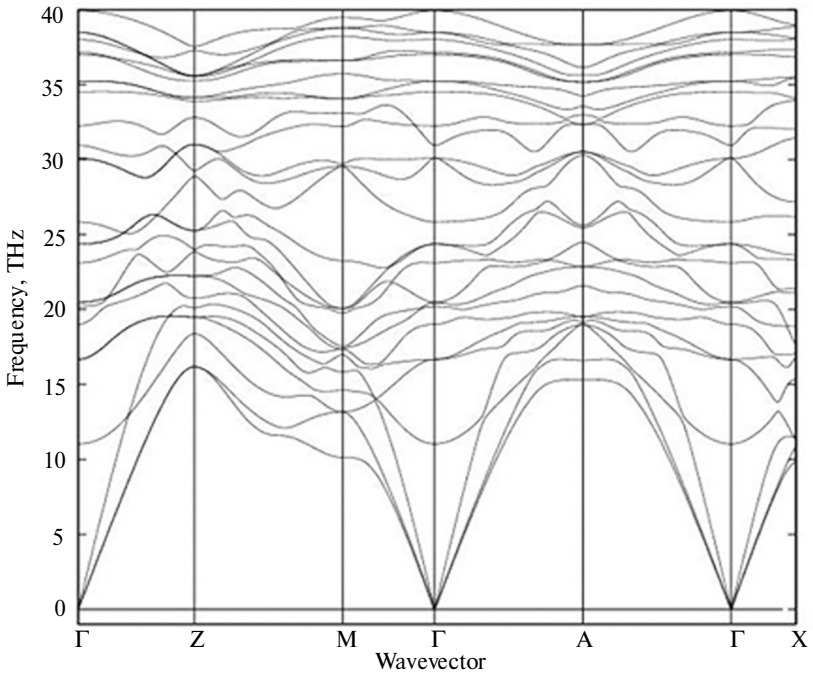

Fig. 3. Phonon dispersion curves of *tP*9-carbon. The absence of imaginary frequencies demonstrates dynamical stability.

Table 1. Bader charges and volumes in *tP*9 carbon. Space group $P\bar{4}$, lattice parameters $a = b = 4.560$ Å and $c = 2.556$ Å

Position	*x*	*y*	*z*	Bader charge	Bader volume, Å^3
C_g	0.0000	0.0000	0.0000	–0.0580	6.8912
C_{h1}	0.2881	0.7804	0.2232	–0.0275	5.9987
C_{h2}	0.8394	0.5307	0.2662	+0.0423	5.4811

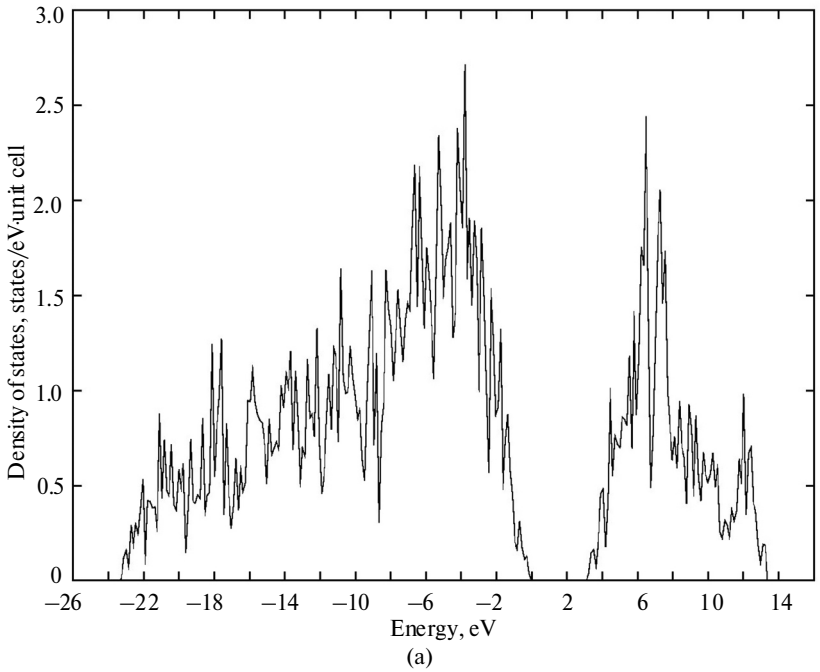

Fig. 4. Density of states (a) and band structure (b) of *tP*9-carbon at 0 GPa, computed with the HSE06 hybrid functional.

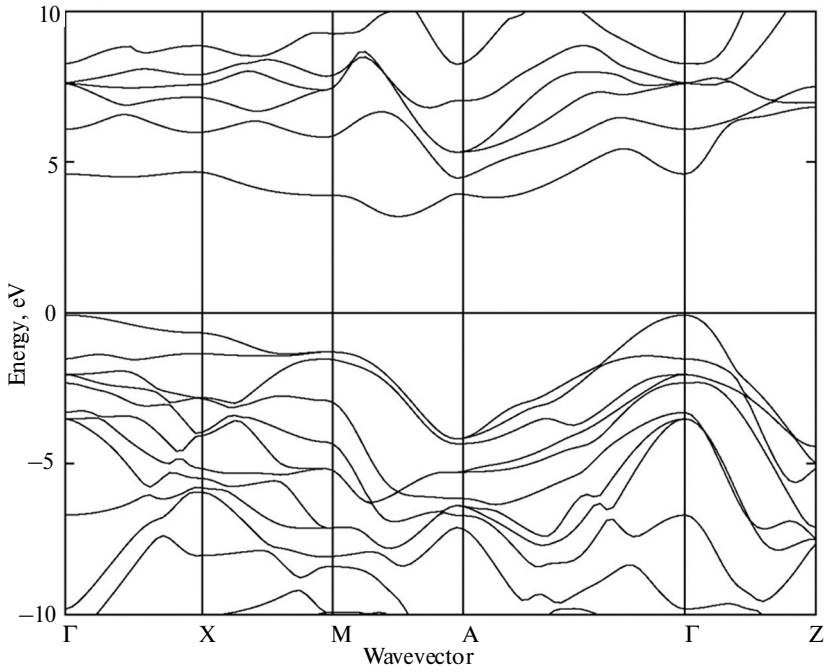

(b)

Fig. 4. (Contd.)

3.2. Optimization of the Host–Guest Ratio—Exploring Possible Incommensurability

Since most host–guest structures of metals are found to be incommensurate, we decided to explore this possibility here. To this end, we used the method of Arapan et al. [22] and performed calculations for a set of commensurate approximants with different C_g/C_h ratios (C_g and C_h are the numbers of guest and host cells in an approximant supercell, respectively). Because the total energy is a continuous function of structural parameters, after interpolating the energy as a function of C_g/C_h, one can obtain the minimum energy and the C_g/C_h ratio corresponding to it. If C_g/C_h is an irrational number, this would indicate an incommensurate modulation of the structure. Figures 5 and 6 show the calculated energies and enthalpies of various commensurate structures; on can see that the commensurate structure with the $C_g/C_h = 2/3$, containing 26 atoms in the unit cell, is energetically optimal. Parameters of this structure are given in Table 2.

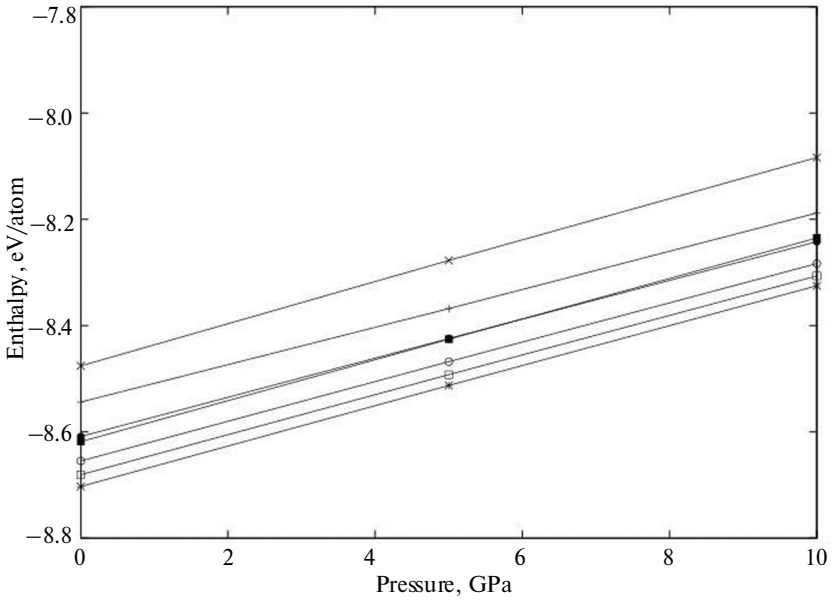

Fig. 5. Enthalpies of various commensurate analogues as a function of pressure: 1*1 (+), 1*2 (×), 2*3 (∗), 3*4 (□), 3*5 (■), 4*5 (○), 9*10 (●).

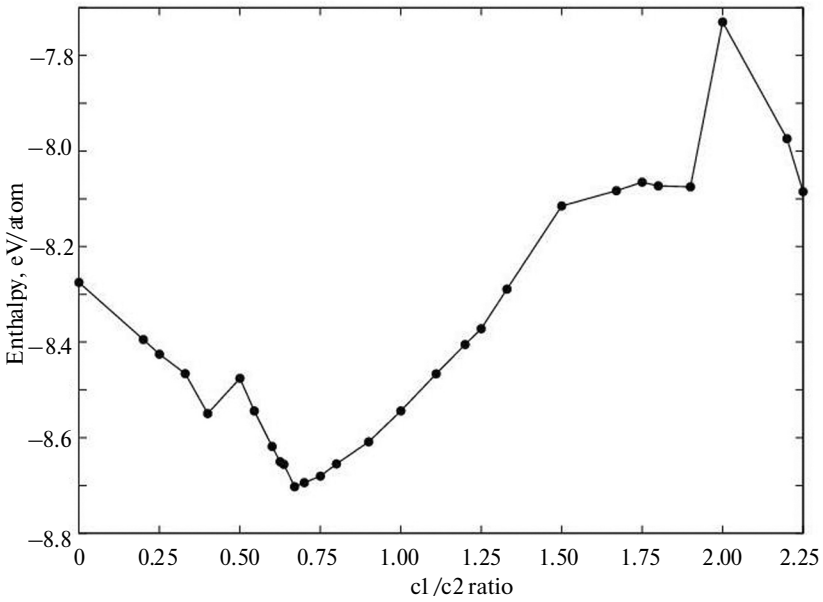

Fig. 6. Total energies of various commensurate structures. Outside the range c1/c2 ∈ [0.5, 1.5] the structure spontaneously changes into very different topologies.

Table 2. Bader charges and volumes in the 2/3 modulated structure. Space group $P4_2/m$, lattice parameters $a = b =$ 4.600 Å, $c = 7.499$ Å

Position	x	y	z	Bader charge	Bader volume, Å^3
$C_{g\text{-}2a}$	0.0000	0.0000	0.0000	−0.0669	7.5665
$C_{h1\text{-}8k}$	0.2672	0.8027	0.0721	+0.0337	6.1236
$C_{h2\text{-}8k}$	0.8319	0.5138	0.0892	−0.0126	5.9542
$C_{h3\text{-}8k}$	0.6413	0.6073	0.2500	−0.0044	5.9274

The new 2/3 structure is more stable than *tP*9-carbon by 0.16 eV/atom. It is also dynamically stable, as we can see in Fig. 7. Its lattice parameters are slightly different from those of *tP*9-carbon: $a = b = 4.600$ Å, but $c =$ 7.499 Å, approximately three times the value of the c-parameter of the 1/1 structure.

The band structure of the 2/3-structure is shown in Fig. 8, and electronic densities of states computed with PBE and HSE06 are shown in Fig. 9. The computed HSE06 band gap is 4.1 eV (much higher than 3.0 eV computed for the *tP*9 structure). Its hardness is computed to be 60.6 GPa using model [16] and 70.6 with model [42], the computed bulk modulus is 383.6 GPa. The density of this phase of carbon is 3.25 g/cm^3.

3.3. SiC_8 Compound

We have investigated the possibility of replacing one of the sublattices with another element. When we replaced the guest carbon atom by a larger silicon atom, the structure remained dynamically stable (Fig. 10). Just like the host, the guest atoms are 4-coordinate with a noticeably larger bond lengths of 1.70 Å (the normal single C–C bond length is 1.54 Å). Thus, it is natural to place a large atom, such as Si, in the guest sublattice, and we did it for the parent 1/1 structure. The structure has space group $P\bar{4}$, with two independent 4h Wyckoff positions occupied in the host sublattice by C atoms, with coordinates (0.694, 0.232, 0.241) and (0.165, 0.477, 0.257), and the Si atom in the guest sublattice occupies the 1a site at (0,0,0); the lattice parameters are $a = b =$ 4.830 Å and $c = 2.522$ Å. SiC_8 is found to have interesting physical properties. Its bulk modulus is 361.2 GPa; the hardness computed with model [16] is 46.2 GPa, i.e., the material is superhard. The HSE06 [41] band gap is 1.8 eV. This result is interesting for absorption of solar light—with possible applications in photocatalysis. Density of states, calculated at different pressures using the HSE06 functional, is shown in Fig. 11. We can see that the band gap slightly increases with pressure—opposite to the normal tendency, but similar to diamond [49]. The density of SiC_8 is 3.49 g/cm^3.

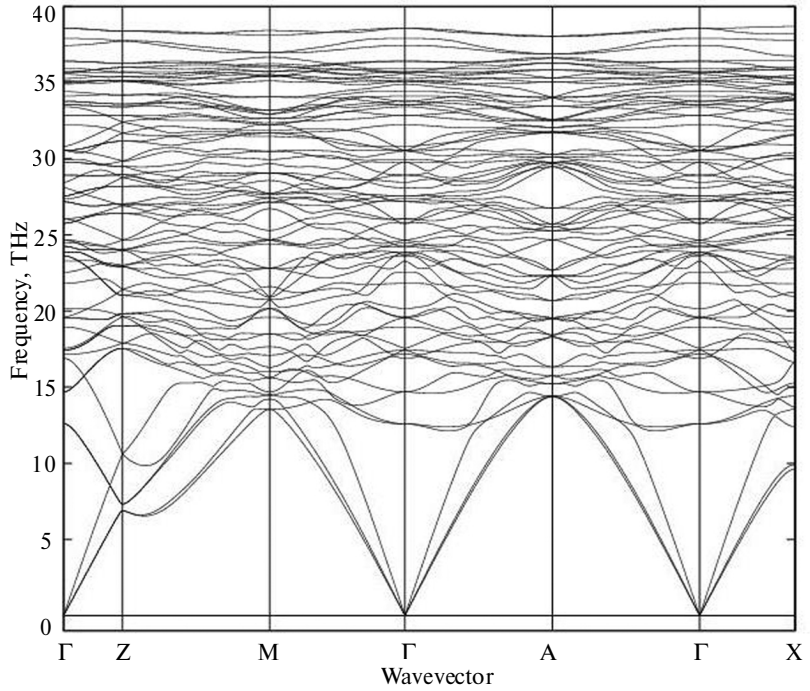

Fig. 7. Phonon dispersion curves of the 2/3 commensurate modulation of *tP*9C carbon.

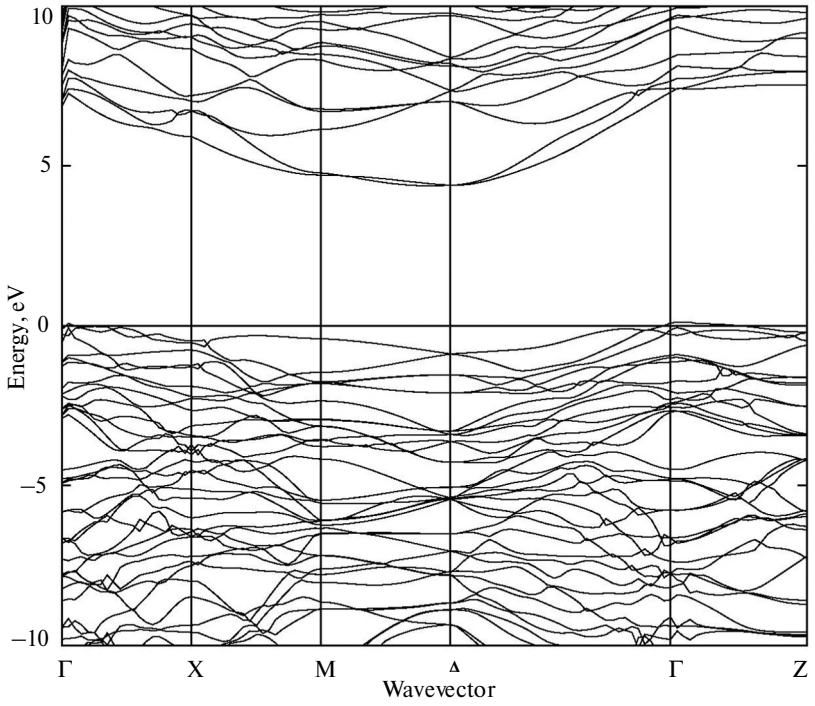

Fig. 8. HSE06 band structure of the 2/3 modulated variant of the *tP*9 structure.

It is interesting to compare energy of the isochemical mixture of diamond-like Si (the ground state of Si) and diamond C with the energy of our SiC_8 structure. We find that SiC_8 is 0.27 eV/atom less stable than the isochemical mixture of diamond-structured Si and C. The enthalpy of formation from true ground states of the elements, diamond-like Si and C-graphite, is 0.38 eV/atom.

In the Si–C system, there is a stable phase SiC. We have explored the enthalpy of formation of SiC_8 from a mixture SiC + 7C(graphite), and the resulting value is 0.44 eV/atom.

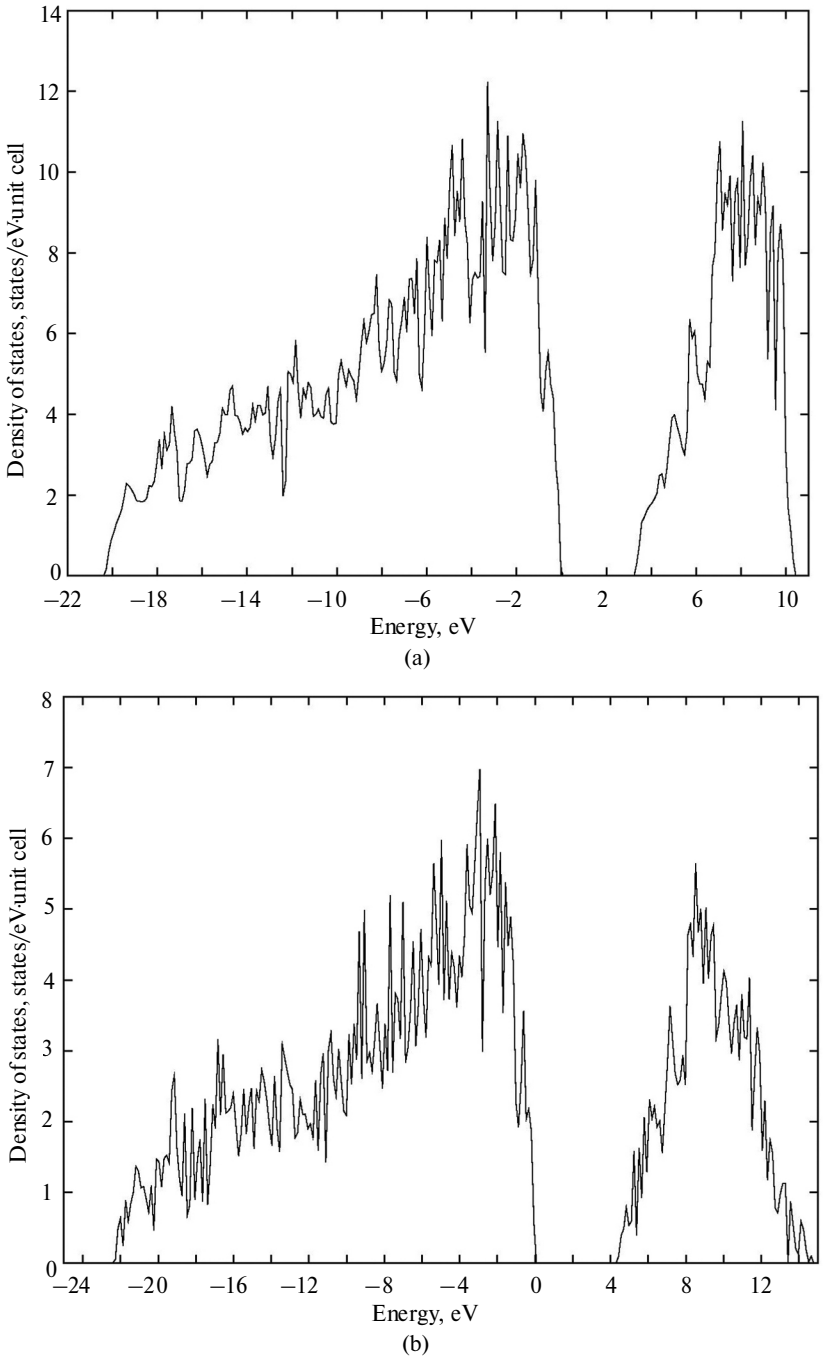

Fig. 9. Electronic density of states of the 2/3 structure computed using PBE (a) and HSE06 (b) functionals.

Results of Bader analysis are shown in Table 3. One can see a large positive charge on the Si atom.

Table 3. Bader charges and in the hypothetical compound SiC_8. Space group $P\bar{4}$, lattice parameters $a = b = 4.830$ Å and $c = 2.522$ Å

Position	x	y	z	Bader charge	Bader volume, Å^3
Si	0.0000	0.0000	0.0000	+2.3008	5.4078
C_{h1}	0.6944	0.2326	0.2417	−0.5854	7.5396
C_{h2}	0.1640	0.4769	0.2575	+0.0102	5.8274

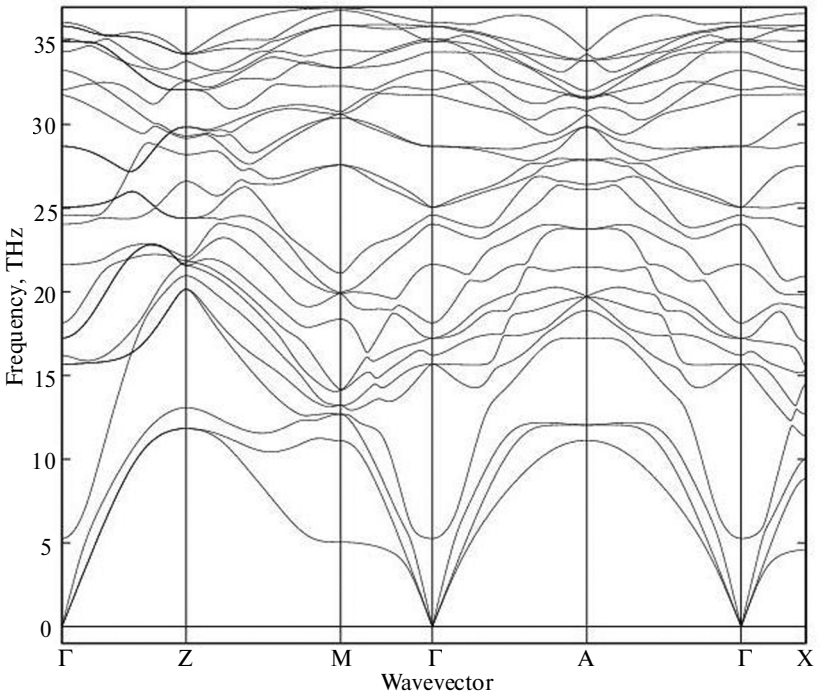

Fig. 10. Phonon dispersion curves of SiC_8.

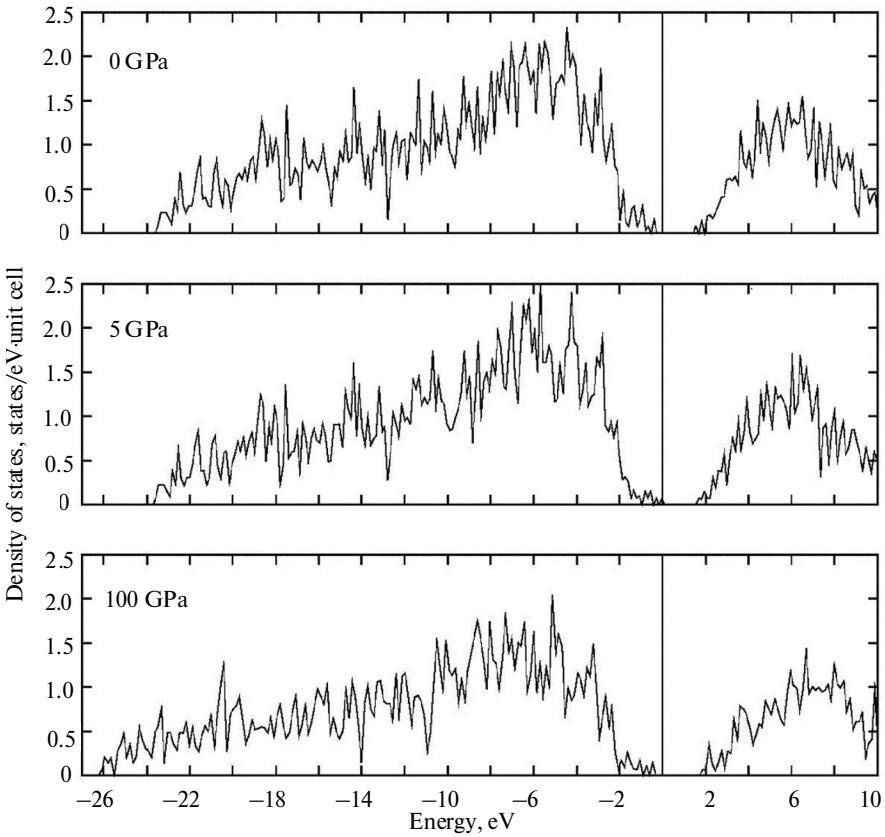

Fig. 11. The density of states for host–guest SiC_8 compound at 0, 5, 100 GPa computed using the HSE06 hybrid functional.

4. CONCLUSIONS

We report a novel family of metastable host–guest structures of carbon, the simplest prototype of which is the tetragonal *tP*9 structure with 9 atoms in the unit cell. This structure consists of host (8 atoms/cell) and

guest (1 atom/cell) sublattices, the guest forming 1D-chains running along the channels of the host structure. It shares similarities with well-known Ba-IV and Rb-IV host–guest structures, which become stable at elevated pressures [22], and exemplifies an extension of such structures to low-coordinate topologies. Theoretical calculations showed that it is a semiconductor with a band gap of 3.0 eV at 0 GPa and hardness 70–73 GPa. This structure is 0.55 eV/atom less stable than diamond at atmospheric pressure.

Looking at a series of modulations of this host–guest structure, it have been found that the 2/3 modulation gives the lowest energy, lowering the energy by 0.16 eV/atom. This optimal host–guest structure contains 26 atoms in the unit cell and is 0.52 eV/atom less stable than graphite, and 0.39 eV/atom less stable than diamond. Its hardness is 61–71 GPa, and its band gap is 4.1 eV.

By replacing carbon atoms in the guest sublattice with Si atoms, a hypothetical SiC_8 compound has been obtained, which is 0.27 eV/atom higher in energy than the isochemical mixture of C-diamond and diamond-type Si. This material is predicted to have interesting properties—hardness of 46 GPa and band gap of 1.8 eV.

These results show that host–guest structures may appear, at least as metastable phases, not only in metals, but also in non-metallic elements, and may have interesting properties. Such phases, or substitution compounds based on them, may be synthesizable.

We thank the National Science Foundation (EAR-1114313, DMR-1231586), DARPA (Grants No. W31P4Q1310005 and No. W31P4Q1210008), and the Government (No. 14.A12.31.0003) and the Ministry of Education and Science of Russian Federation (Project No. 8512) for financial support.

REFERENCES

1. Heimann, R.B., Evsyukov, S.E., and Koga, Y., Carbon allotropes: a suggested classification scheme based on valence orbital hybridization, *Carbon*, 1997, vol. 35, pp. 1654–1657.
2. Iijima, S., Helical microtubules of graphitic carbon, *Nature*, 1991, vol. 354, pp. 56–58.
3. Ekimov, E.A., Sidorov, V.A., Bauer, E.D., et al., Superconductivity in diamond, *Ibid.*, 2004, vol. 428, pp. 542–545.
4. Meyer, J.C., Geim, A.K., Katsnelson, M.I., et al., The structure of suspended graphene sheets, *Ibid.*, 2007, vol. 446, pp. 60–63.
5. Wang, X., Scandolo, S., and Car, R., Carbon phase diagram from ab initio molecular dynamics, *Phys. Rev. Lett.*, 2005, vol. 95, art. 185701.
6. Mao, W.L., Mao, H.K., Eng, P.J., et al., Bonding changes in compressed superhard graphite, *Science*, 2003, vol. 302, pp. 425–427.
7. Buchnum, M.J. and Hoffman, R., A hypothetical dense 3,4-connected carbon net and related B_2C and CN_2 nets built from 1,4-cyclohexadienoid units, *J. Am. Chem. Soc.*, 1994, vol. 116, pp. 11456–11464.
8. Winkler, B., Pickard, C.J., Milman, V., et al., Prediction of a nanoporous sp^2-carbon framework structure by combining graph theory with quantum mechanics, *Chem. Phys. Lett.*, 1999, vol. 312, pp. 536–541.
9. Li, Q., Ma, Y., Oganov, A.R., et al., Superhard monoclinic polymorph of carbon, *Phys. Rev. Lett.*, 2009, vol. 102, art. 175506.
10. Ribeiro, F.J., Tangney, P., Louie, S.G., et al., Structural and electronic properties of carbon in hybrid diamond-graphite structures, *Phys. Rev. B*, 2005, vol. 72, art. 214109.
11. Wang, Z.W., Zhao, Y.S., Tait, K., et al., A quenchable superhard carbon phase synthesized by cold compression of carbon nanotubes, *Proc. Natl. Acad. Sci.*, 2004, vol. 101, pp. 13699–13702.
12. Pickard, C.J. and Needs, R.J., Hypothetical low-energy chiral framework structure of group 14 elements, *Phys. Rev. B*, 2010, vol. 81, art. 014106.
13. Umemoto, K., Wentzcovitch, R.M., Saito, S., et al., Body-centered tetragonal C_4: A viable sp^3 carbon allotrope, *Phys. Rev. Lett.*, 2010, vol. 104, art. 125504.
14. Hoffmann, R., Hughbanks, T., and Kertesz, M., A hypothetical metallic allotrope of carbon, *J. Am. Chem. Soc.*, 1983, vol. 105, pp. 4831–4832.
15. Zhu, Q., Oganov, A.R., Salvado, M., et al., Denser than diamond: ab initio search for superdense carbon allotropes, *Phys. Rev. B*, 2011, vol. 83, art. 193410.
16. Lyakhov, A.O. and Oganov, A.R., Evolutionary search for superhard materials applied to forms of carbon and TiO_2, *Ibid.*, 2011, vol. 84, art. 092103.
17. Zhu, Q., Zeng, Q., and Oganov, A.R., Systematic search for low-enthalpy sp^3 carbon allotropes using evolutionary metadynamics, *Ibid.*, 2011, vol. 85, art. 201407.
18. McMahon, M.I. and Nelmes, R.J., High-pressure structures and phase transformations in elemental metals, *Chem. Soc. Rev.*, 2006, vol. 35, pp. 943–963.
19. Nelmes, R.J., Allan, D.R., Mcmahonet, M.I., et al., Self-hosting incommensurate structure of barium-IV, *Phys. Rev. Lett.*, 1999, vol. 83, pp. 4081–4084.

20. Reed, S.K. and Ackland, G.J., Theoretical and computational study of high-pressure structures in barium, *Ibid.*, 2000, vol. 84, pp. 5580–5584.

21. McMahon, M.I., Degtyareva, O., and Nelmes, R.J., Pressure dependent incommensuration in Rb-IV, *Ibid.*, 2001, vol. 87, art. 055501.

22. Arapan, S., Mao H.K., and Ahuja, R., Prediction of incommensurate crystal structure in Ca at high pressure, *Proc. Natl. Acad. Sci.*, 2008, vol. 52, pp. 20627–20630.

23. Oganov, A.R., Ma, Y.M., Xu, Y., et al., Exotic behavior and crystal structures of calcium under pressure, *Ibid.*, 2010, vol. 107, pp. 7646–7651.

24. McMahon, M.I., Degtyareva, O., and Nelmes, R.J., Ba-IV-type incommensurate crystal structure in group-V metals, *Phys. Rev. Lett.*, 2000, vol. 85, pp. 4896–4899.

25. Degtyareva, O., McMahon, M.I., and Nelmes, R.J., Pressure-induced incommensurate-to-incommensurate phase transition in antimony, *Phys. Rev. B*, 2004, vol. 70, art. 18419.

26. Fujihisa, H., Akahama, Y., Kawamura, H. et al., Incommensurate structure of phosphorus phase IV, *Phys. Rev. Lett.*, 2007, vol. 98, art. 175501.

27. Hejny, C. and McMahon, M.I., Large structural modulations in incommensurate Te-III and Se-IV, *Ibid.*, 2003, vol. 91, art. 215502.

28. McMahon, M.I, Hejny, C., Loveday, J.S., et al., Confirmation of the incommensurate nature of Se-IV at pressures below 70 GPa, *Phys. Rev. B*, 2004, vol. 70, art. 054101.

29. Hejny, C., Lundegaard, L.F., Falconi, S., et al., Incommensurate sulfur above 100 GPa, *Ibid.*, 2005, vol. 71, art. 020101.

30. Pickard, C.J. and Needs, R.J., Aluminum at terapascal pressures, *Nat. Mater.*, 2010, vol. 9, pp. 624–627.

31. Oganov, A.R. and Glass, C.W., Crystal structure prediction using ab initio evolutionary techniques: principles and applications, *J. Chem. Phys.*, 2006, vol. 124, art. 244704.

32. Oganov, A.R., Lyakhov, A.O., and Valle, M., How evolutionary crystal structure prediction works—and why, *Acc. Chem. Res.*, 2011, vol. 44, pp. 227–237.

33. Lyakhov, A.O., Oganov, A.R., Stokes, H.T., et al., New developments in evolutionary structure prediction algorithm USPEX, *Comp. Phys. Comm.*, 2013, vol. 184, pp. 1172–1182.

34. Hohenberg, P. and Kohn, W., Inhomogeneous electron gas, *Phys. Rev. B*, 1964, vol. 136, pp. 864–871.

35. Kohn, W. and Sham, L.J., Self-consistent equations including exchange and correlation effects, *Phys. Rev. A*, 1965, vol. 140, pp. 1133–1138.

36. Perdew, J.P., Burke, K., and Ernzerhof, M., Generalized gradient approximation made simple, *Phys. Rev. Lett.*, 1996, vol. 77, pp. 3865.

37. Blochl, P.E., Projector augmented-wave method, *Phys. Rev. B*, 1994, vol. 50, pp. 17953–17978.

38. Kresse, G. and Joubert, D., From ultrasoft pseudopotentials to the projector augmented-wave method, *Ibid.*, 1999, vol. 59, pp.1758–1775.

39. Kresse, G. and Furthmller, J., Efficient iterative schemes for ab initio total-energy calculations using a plane-wave basis set, *Ibid.*, 1996, vol. 54, pp. 11169–11186.

40. Togo, A., Oba, F., and Tanaka, I., First-principles calculations of the ferroelastic transition between rutile-type and $CaCl_2$-type SiO_2 at high pressures, *Ibid.*, 2008, vol. 78, art. 134106.

41. Heyd, J., Scuseria, G.E., and Ernzerhof, M., Hybrid functionals based on a screened Coulomb potential, *J. Chem. Phys.*, 2006, vol. 124, art. 219906.

42. Bader, R.F.W., *Atoms in molecules. A quantum theory*, Oxford: Oxford University Press, 1990.

43. Tang, W., Sanville, E., and Henkelman, G., A grid-based Bader analysis algorithm without lattice bias, *J. Phys.: Condens. Matter*, 2009, vol. 21, art. 084204.

44. Chen, X.-Q., Niu, H., Li, D., et al., Modeling hardness of polycrystalline materials and bulk metallic glasses, *Intermetallics*, 2011, vol. 19, pp. 1275–1281.

45. Hill, R., The elastic behavior of a crystalline aggregate, *Proc. Phys. Soc. London*, 1952, vol. 65, pp. 349–354.

46. Voigt, W., *Lehrbuch der Kristallphysik*, Leipzig: Verl. von B.G. Teubner, 1928.

47. Reuss, A., Berechnung der Fliessgrenze von Mischkristallen auf Grund der Plastizitatsbedingung fur Einkristalle, *Z. Angew. Math. Mech.*, 1929, vol. 9, pp. 49–58.

48. Oganov, A.R, Chen, J., Gatti, C., et al., Ionic high-pressure form of elemental boron, *Nature*, 2009, vol. 457, pp. 863–867.

49. Fahy, S., Chang, K.J, and Louie, S.G., Pressure coefficients of band gaps of diamond, *Phys. Rev. B*, 1987, vol. 35, pp. 5856–5859.